O3M SAF VALIDATION REPORT

Validated products:

Identifier	Name	Acronym
O3M-10	Offline Total Formaldehyde	OTO/HCHO

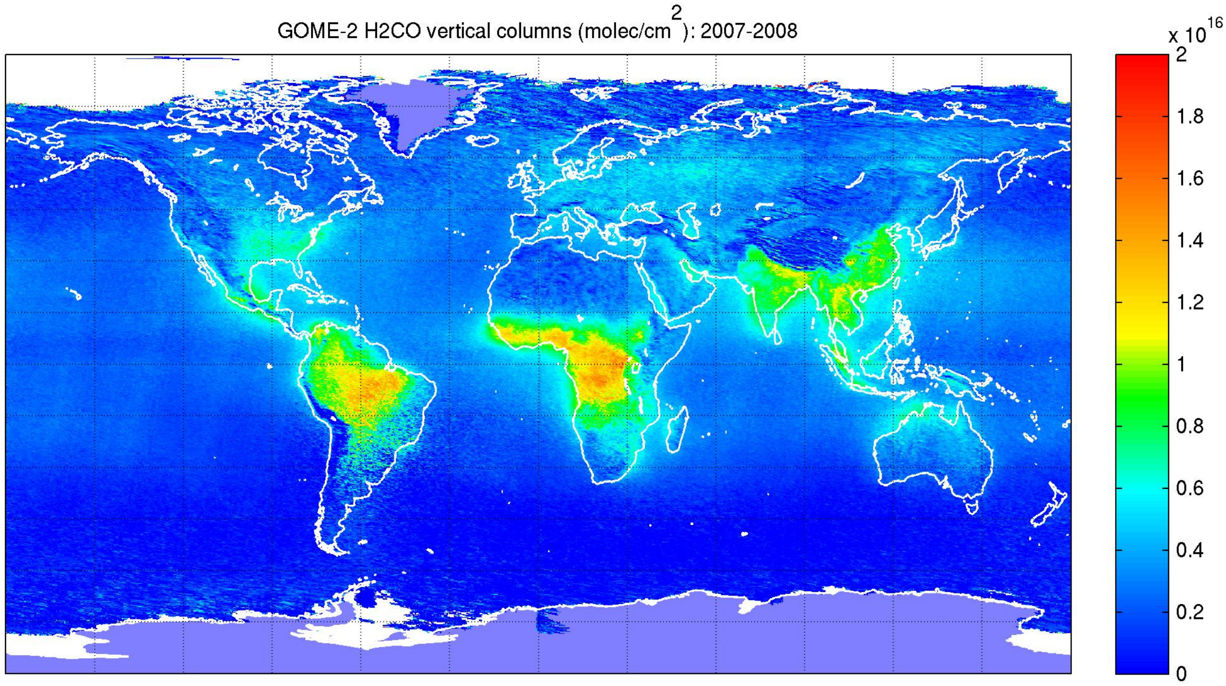

Authors:

Name	Institute
Isabelle De Smedt	Belgian Institute for Space Aeronomy
Michel Van Roozendael	Belgian Institute for Space Aeronomy
Nan Hao	German Aerospace Center
Pieter Valks	German Aerospace Center

Reporting period: January 2007 – August 2009
Input data versions: GOME-2 Level 1B version 4.x
Data processor versions: GDP 4.4, UPAS version 1.4.0

Validation of GOME-2 H_2CO total columns – ORR B3

ACRONYMS AND ABBREVIATIONS

AMF	Air Mass Factor, or optical enhancement factor
BIRA-IASB	Belgian Institute for Space Aeronomy
BrO	bromine monoxide
DLR	German Aerospace Centre
DOAS	Differential Optical Absorption Spectroscopy
ENVISAT	Environmental Satellite
ERS-2	European Remote Sensing Satellite -2
ESA	European Space Agency
EUMETSAT	European Organisation for the Exploitation of Meteorological Satellites
FMI	Finnish Meteorological Institute – Arctic Research Centre
GB-DOAS	Ground-based DOAS instruments
GDP	GOME Data Processor
GOME	Global Ozone Monitoring Experiment
H_2CO	Formaldehyde
IMF	Remote Sensing Technology Institute
OCRA	Optical Cloud Recognition Algorithm
NDACC	Network for the Detection of Atmospheric Composition Change
O3M-SAF	Ozone and Atmospheric Chemistry Monitoring Satellite Application Facility
OMI	Ozone Monitoring Instrument
ROCINN	Retrieval of Cloud Information using Neural Networks
SCD	Slant Column Density
SCIAMACHY	Scanning Imaging Absorption spectroMeter for Atmospheric CHartography
SZA	Solar Zenith Angle
TEMIS	Tropospheric Emission Monitoring Internet Service
UPAS	Universal Processor for UV/VIS Atmospheric Spectrometers
VCD	Vertical Column Density
WMO	World Meteorological Organization

A. INTRODUCTION

A.1. Scope of this document

The present document reports on the verification and initial validation of MetOp-A GOME-2 H_2CO total column product OTO/HCHO over the January 2007 - August 2009 time period, produced by the GOME Data Processor (GDP) version 4.4 operated at DLR on behalf of EUMETSAT. This report includes verification work performed using the BIRA-IASB scientific retrieval tool synchronized on the GDP settings, as well as comparisons with GOME, SCIAMACHY and ground-based measurements.

A.2. Preliminary notes

H_2CO total columns as generated with GDP algorithm version 4.4 represent a new GOME-2 O3M-SAF product, generated within the UPAS operational environment system at DLR.

The aim of the present document is first to report on the status of the verification of the GOME-2 H_2CO column against a synchronised scientific algorithm available at BIRA-IASB. For this exercise, H_2CO retrieval settings developed at BIRA-IASB for the scientific product, adapted to the constraints of the operational environment of the GDP version 4.4, are being used. The consistency of this H_2CO product is then explored by performing various comparisons with existing correlative data sets, including scientific data sets from GOME and SCIAMACHY. Ground-based H_2CO column measurements available in Beijing, Cabauw and Reunion Island are also used in an attempt to further document the geophysical consistency of the GOME-2 H_2CO product.

Reported validation studies were carried out at the Belgian Institute for Space Aeronomy (IASB-BIRA, Brussels, Belgium) and at DLR Remote Sensing Technology Institute (DLR-IMF, Oberpfaffenhofen, Germany) in the framework of EUMETSAT Satellite Application Facility on Ozone and Atmospheric Chemistry Monitoring (O3M-SAF)

A.3. Plan of this document

This document is divided in five main parts, addressing respectively the description of the retrieval settings applied for the H_2CO product, the verification of the slant columns, the verification of air mass factors and the vertical columns, comparisons against satellite data and comparisons against ground-based measurements. This is followed by concluding remarks and perspectives for future work.

A.4. Applicable O3MSAF Documents

[ATBD] Algorithm Theoretical Basis Document for GOME-2 Total Column Products of Ozone, NO_2, SO_2, BrO, H_2O, HCHO, OClO, tropospheric NO_2 and Cloud Properties, DLR/GOME-2/ATBD/01/2B, Valks, P., Loyola D., Hao N., Rix M., Slijkhuis S., 2009.

[PUM] Product User Manual for GOME Total Column Products of Ozone, NO_2, SO_2, BrO, H_2O, HCHO, OClO, tropospheric NO_2 and Cloud Properties, DLR/GOME/PUM/01, Rev. 2/B, Loyola D., Zimmer W., Kiemle S., Valks P., Emmadi S., 2009.

[PRD] Product Requirements Document, SAF/O3M/FMI/RQ/PRD/001/Rev. 06, D. Hovila, J., S. Kiemle, O. Tuinder, H. Joench-Soerensen, F. Karcher, 2008.

A.5. Technical information

GOME-2 product name H_2CO total column (OTO/HCHO)

Validation reporting period January 2007 – August 2009

Level-2 processor version GDP 4.4, UPAS version 1.4.0

Input GOME-2 Level-1B data version table

Start Date	Start Orbit	Level 1B Version
Jan 04, 2007	1093	4.0
Jan 07, 2009	11521	4.1.0
Apr 07, 2009	12796	4.2.0
Aug 18, 2009	14687	4.3.0

B. SETTINGS FOR H_2CO COLUMN RETRIEVAL FROM GOME-2

B.1. Experience from ERS-2 GOME and SCIAMACHY

Despite the relatively large abundance of H_2CO in the atmosphere (on the order of 10^{16} molec/cm^2) and its well defined absorption bands, the fitting of H_2CO slant columns in earthshine radiances is a challenge because of the low optical density of H_2CO compared to other UV absorbers. The typical H_2CO optical density is about 2.5 times smaller than for BrO and up to 50 times smaller than for NO_2. Therefore, the detection of H_2CO is limited by the signal to noise ratio of the measured radiance and by possible spectral interferences due to other molecules absorbing in the same fitting interval, mainly ozone.

H_2CO columns have been retrieved from ERS-2 GOME and ENVISAT SCIAMACHY instruments and settings used for these two instruments are documented in the literature (De Smedt et al., 2008). Slant columns are fitted in the 328.5–346nm wavelength range. This choice of the fitting interval minimizes uncertainties due to a polarization anomaly affecting the SCIAMACHY spectra around 350 nm, and to a major absorption band of the O_4 collision complex (centred near 360 nm). Furthermore, it decreases fitting residuals in tropical areas and reduces noise over the oceans (De Smedt et al., 2008). The H_2CO absorption cross sections used in the DOAS fit are those of Meller et al. (2000). The fitting procedure includes reference spectra for other interfering species (O_3, NO_2, BrO, OClO). The Ring effect is corrected according to Chance and Spurr (1997). A linear intensity offset correction is further applied as well as a polynomial closure term of order 5. In order to minimise the impact of the GOME diffuser plate related artefact (Richter and Wagner, 2001) and to minimize fitting residuals, daily radiance spectra are used as the I_0 reference. These are selected in a region of the equatorial Pacific Ocean where the formaldehyde column is assumed to be low and stable in time (Stavrakou et al., 2008). To reduce the impact of fitting artefacts due to unresolved spectral interferences with ozone and BrO absorptions, an absolute normalisation is applied on a daily basis using the reference sector method (De Smedt et al., 2008). The reference sector is chosen in the central Pacific Ocean (140°–160° W), where the only significant source of H_2CO is the CH_4 oxidation. The latitudinal dependency of the H_2CO slant columns in the reference sector is modelled by a polynomial, subtracted from the slant columns and replaced by the H_2CO background taken from the tropospheric 3-D-CTM IMAGES (Stavrakou et al., 2009a) in the same region. The SCIAMACHY H_2CO columns are found to produce H_2CO slant columns in good agreement with GOME (De Smedt et al., 2008).

B.2. Choice of H_2CO slant column settings for GOME-2

Although different fitting windows have been tested, the best results and consistency with the previous H_2CO observations have been found in the same interval as for GOME and SCIAMACHY (328.-5-346 nm). The same high–resolution cross-sections datasets have been used for the 3 satellite instruments. Using radiance spectra as reference, the noise on the individual GOME-2 H_2CO measurements was found to be consistent with the ground pixel size of the instruments (approx. 40x80 km^2 for GOME-2, 30x60 km² for SCIAMACHY and 40x320 km^2 for GOME). Tests have been performed using daily solar irradiance spectra as reference for GOME-2. The results showed that the quality of the H_2CO slant columns is equivalent when using irradiances as I_0 reference, even if the fitting residuals are 10 to 20% higher. Therefore, it has been decided to use solar irradiances as reference for the GDP product and also for the scientific product developed at BIRA-IASB. In any case, the reference sector correction is needed to further correct for fitting interferences with the ozone absorption. The fit residuals of the slant columns increase with solar zenith angles. Therefore, a SZA of 70° is taken as an upper limit for the selection of the satellite pixels. The detailed DOAS settings used for GOME-2 H_2CO slant column retrievals are given in Table1.

Table 1. DOAS settings used for GOME-2 H_2CO slant column verification

Fitting interval	328.5-346 nm
Sun reference	Sun irradiance from file
Wavelength calibration	Wavelength calibration of sun reference optimized by NLLS adjustment on convolved Chance and Spurr solar lines atlas
Absorption cross-sections	
H_2CO	Meller et al., 2000, 298°K
Ozone	Brion et al. 1998, 228°K + 243°K
BrO	Fleischmann et al., 223°K
NO_2	Vandaele, 2002, 220°K
OClO	Bogumil et al., 2003, 293°K
Ring effect	2 Ring eigenvectors generated using SCIATRAN
Polynomial	5rd order (6 parameters)
Intensity offset correction	Constant or Linear offset

B.3. Air Mass Factors and Vertical Column Calculation for Formaldehyde

In BIRA-IASB, vertical columns are obtained by dividing the slant columns by air mass factors (AMFs) (Palmer et al., 2001) calculated using scattering weights evaluated from radiative transfer calculations performed with the DISORT code (Mayer and Kylling, 2005). A correction for cloud effects is applied based on the independent pixel approximation (Martin et al., 2002), but aerosols are not explicitly considered in the current version of the dataset. The error due to the cloud correction scheme used in the retrieval is only acceptable for low cloud fraction values, therefore pixels with cloud fractions larger than 0.4 are rejected. The ground albedo is obtained from the GOME climatology of Koelemeijer et al. (2003). Cloud information is provided by the FRESCO+ algorithm (Wang et al., 2008). For the determination of the AMFs, H_2CO vertical profiles are needed a priori. They are provided by the IMAGESv2 global chemistry transport model (Stavrakou et al., 2009a) on a monthly basis and interpolated for each satellite geolocation. Figure 1 presents examples of results of the monthly mean VCD for April 2007.

The same algorithmic steps and a priori profiles from the IMAGESv2 model are used in the GDP 4.4. However, scattering weights are evaluated with the LIDORT 3.3 radiative transfer model and the ground albedo is obtained from the combined TOMS/GOME climatology. As described in Boersma et al. (2004), the TOMS/GOME climatology is based on a TOMS-derived LER at 380 nm, which has the advantage to offer a better horizontal resolution. To account for the wavelength dependence of the albedo, the TOMS LER values are scaled to the ratio of the GOME climatologies at both wavelengths 380 nm and 335 nm. In this way, the strengths of both data sets are combined: the long duration of the TOMS record and the spectral information (11 wavelengths) of the shorter GOME record. In the GDP 4.4, the cloud information (cloud fraction, cloud top-pressure and albedo are provided by the OCRA and ROCINN algorithms. To avoid strongly negative vertical columns, the ghost column correction has been switched off for negative slant columns in the GDP 4.4. This is not done in the scientific product (see section D: verification of H_2CO air mass factors and vertical columns).

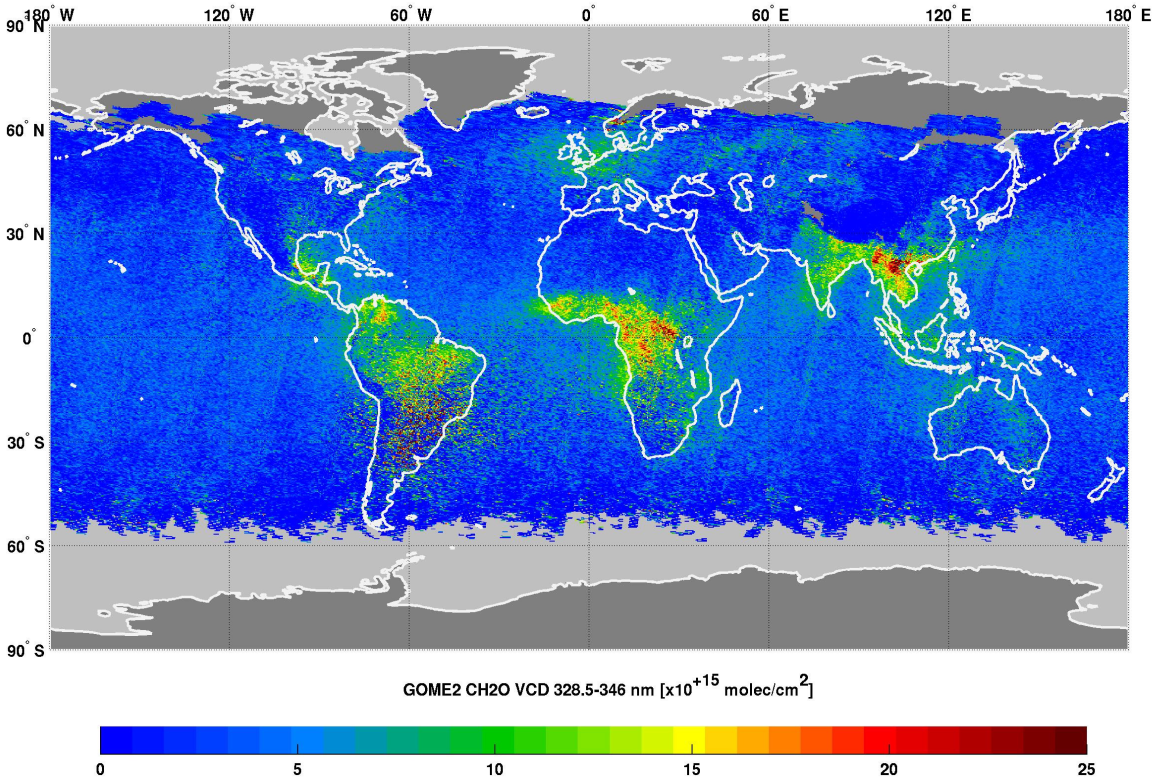

Figure 1. Monthly averaged of GOME-2 H_2CO vertical columns retrieved with the adapted scientific algorithm for April 2007 (using the baseline settings given in Table 1).

C. VERIFICATION OF H_2CO SLANT COLUMNS

In the following sections the consistency of the GDP 4.4 H_2CO column product is investigated from the point of view of (1) the verification (i.e. whether H_2CO retrievals performed with GDP are consistent with scientific retrievals performed using same settings), (2) the comparison against 2 other satellite instruments (GOME and SCIAMACHY), and (3) the comparison against independent ground-based observations from ground-based stations.

For verification purposes, the retrieval software of BIRA-IASB was synchronised with the GDP 4.4 processor, using a common set of slant column retrieval settings, as documented in Table 1. Comparisons between the two processing systems were performed on a limited set of GOME-2 orbits. One orbit (2364) of the 4th April 2007 was selected which is representative for the full range of expected H_2CO concentrations. Results of these comparisons are illustrated in Figure 2. As can be seen, a good level of agreement was obtained, demonstrating the consistency between the two slant column fitting algorithms. The differences in H_2CO SCDs retrieved from GDP processor and BIRA-IASB software show a bias lower than $3x10^{15}$molec/cm² and a standard deviation of 1.6 x 10^{15} molec/cm². The noise on the slant columns, i.e. the standard deviation of the slant columns calculated on a grid of 1°, are found to be equivalent as well as the slant column density errors (Figure 3). After application of the reference sector correction, the offset between the slant columns is reduced to less than $5x10^{14}$ molec/cm², which is well under the noise on the slant columns (Figure 4).

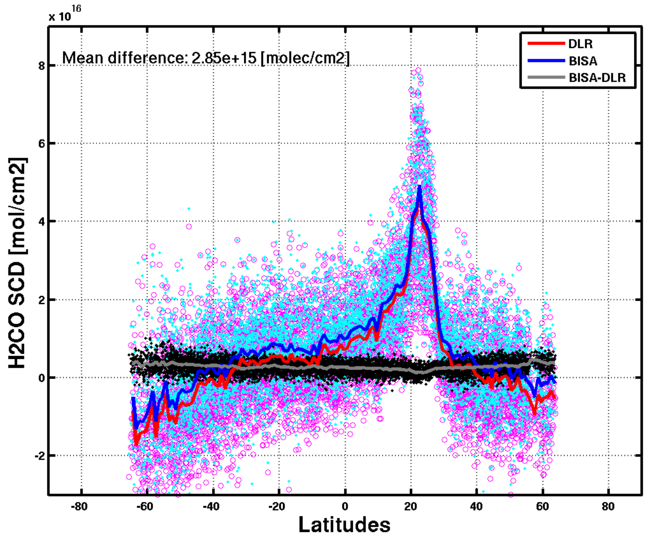

Figure 2. Comparison of H_2CO slant columns retrieved from GDP 4.4 and from the BIRA-IASB scientific algorithm, for one GOME-2 orbit of the 4th April 2007. The black dots correspond to the difference between GDP and BIRA-IASB H_2CO SCDs. DOAS settings were synchronized according to Table 1.

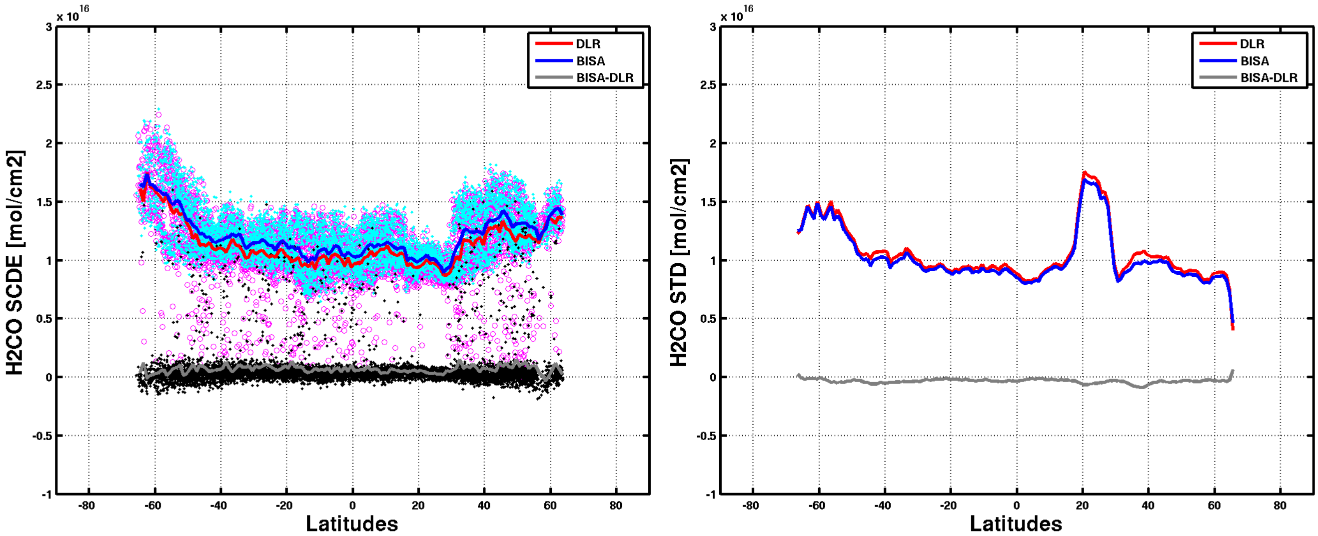

Figure 3. Comparison of H_2CO slant columns errors (first panel) and slant columns standard deviation (second panel) retrieved from GDP 4.4 and from the BIRA-IASB scientific algorithm, for one GOME-2 orbit of the 4th April 2007. The black dots (and the grey line) correspond to the difference between GDP and BIRA-IASB H_2CO retrievals. DOAS settings were synchronized according to Table 1.

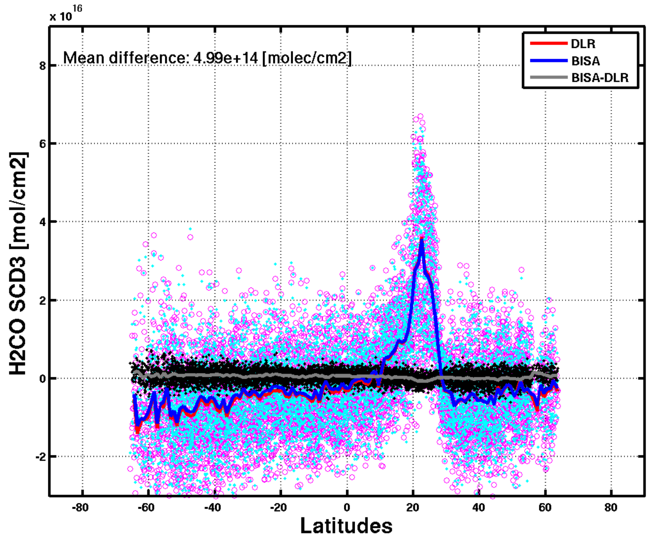

Figure 4. Comparison of H_2CO slant columns retrieved from GDP 4.4 and from the BIRA-IASB scientific algorithm, after the reference sector correction. The black dots correspond to the difference between GDP and BIRA-IASB H_2CO SCDs.

D. VERIFICATION OF H_2CO AIR MASS FACTORS AND VERTICAL COLUMNS

The H_2CO AMFs and vertical columns from the GDP 4.4 have been verified with results from the adapted BIRA-IASB scientific algorithm. The base-line retrieval settings as described in Section B.3 have been used. Table 2 shows the algorithm difference between the BIRA scientific product and GDP 4.4 product.

The comparison for the clear-sky AMF is illustrated on Figure 5. The first panel shows the AMF calculated with the two algorithms, using the GOME surface albedo climatology in the scientific algorithm and the TOMS/GOME surface albedo climatology in GDP 4.4. The second panel shows the same comparison using a common GOME surface albedo data set (Koelemeijer et al., 2002). The comparison of these two surface albedo climatologies is shown on Figure 6 and surface elevation for this orbit can be seen on Figure 7. The difference between the albedo climatology leads to a systematic difference of a little less than 10% in the clear-sky AMFs, resulting in higher vertical columns in the GDP 4.4. The good agreement of the clear-sky AMF in the second panel (mean difference = -0.025 ± 0.09) proves the consistency of the weighting functions calculated respectively with DISORT and LIDORT, a-priori profiles being identical. A slightly different treatment of the ground altitude in the AMF calculation results in the increased clear AMF scatter between 20°N and 40°N, where the altitudes are the highest (Figure 7).

Table 2. Algorithm difference between the BIRA scientific product and GDP 4.4 product

	BIRA	GDP 4.4
Cloud Algorithm	FRESCO+	OCRA/ROCINN
Surface Albedo	GOME climatology	TOMS/GOME climatology*
Ghost Column Correction	For all measurements	For all measurements with positive SCD
Relative Transfer Model	DISORT	LIDORT 3.3

* The TOMS/GOME surface albedo climatology is used in the retrieval of all the GOME-2 (pre)operational trace gas column products.

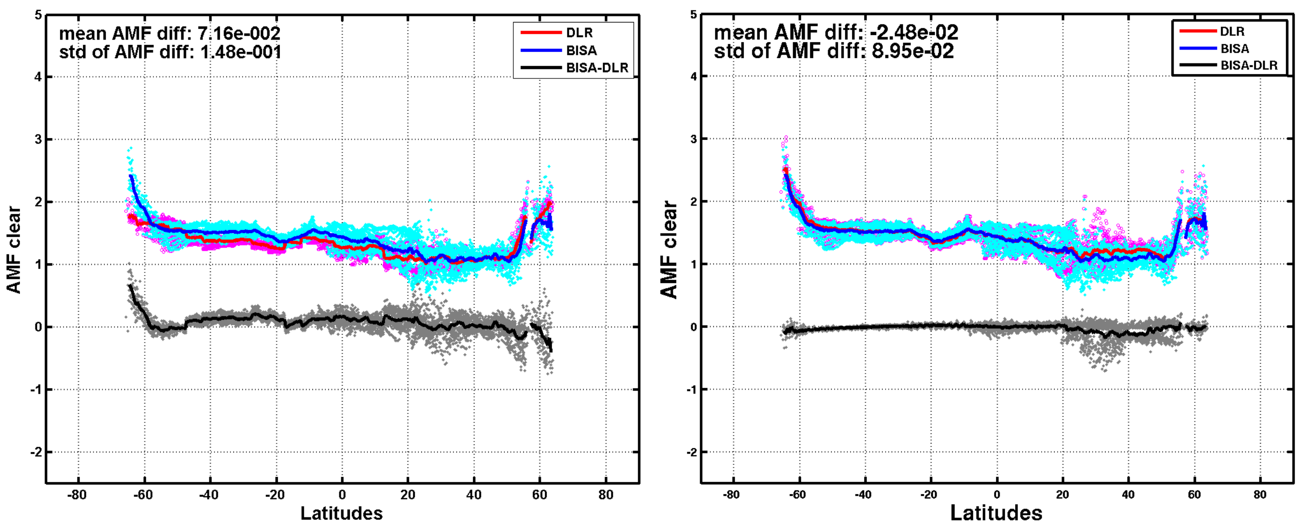

Figure 5. Comparison of clear-sky AMF calculated in the BIRA-IASB scientific algorithm and in the GDP 4.4, for the same GOME-2 orbit of the 4th April 2007. In the first panel, the abledo climatology are

respectively the GOME climatology for the scientific product and the TOMS/GOME climatology for the GDP 4.4. In the second panel, the GOME albedo climatology has been used for the two products.

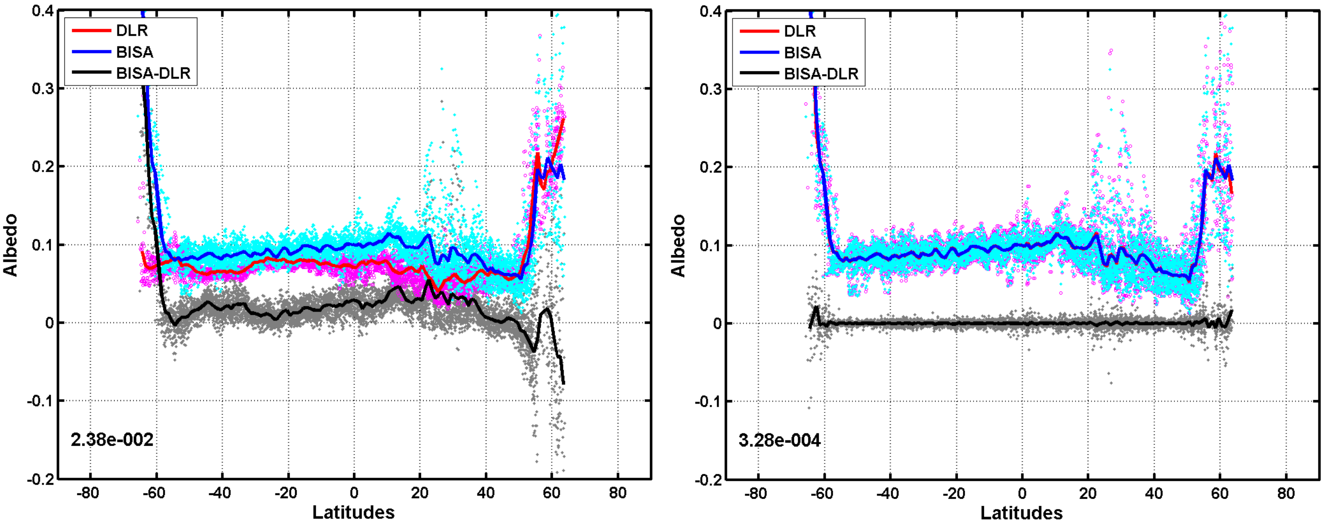

Figure 6. Comparison of the albedo values for the same GOME-2 orbit of the 4th April 2007. In the first panel, the albedo values are taken respectively from the GOME climatology for the scientific product and the TOMS/GOME climatology for the GDP 4.4. In the second panel, the GOME albedo climatology has been used for the two products.

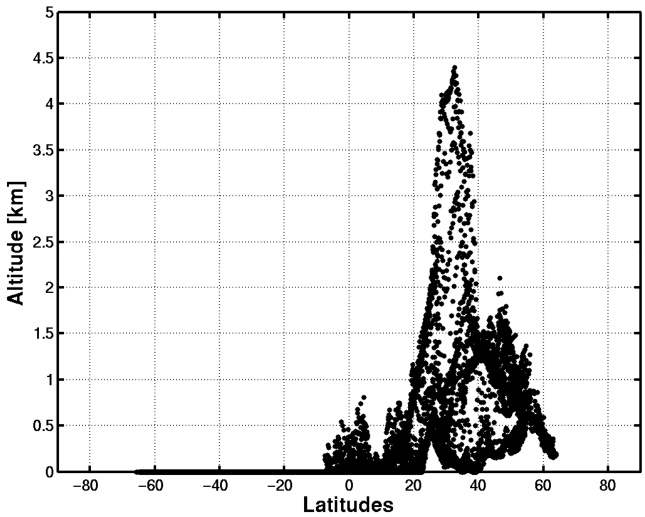

Figure 7. Surface elevation for the same GOME-2 orbit of the 4th April 2007.

For the verification of the cloudy and total AMFs, two different data-sets have been calculated with the BIRA-IASB algorithm using cloud parameters from both FRESCO and OCRA-ROCINN. The first panel of Figure 8 shows the comparison of the total AMF from the BIRA-IASB scientific algorithm (using FRESCO) and the GDP 4.4 (using OCRA-ROCINN). The agreement between both data sets is further improved by using the same cloud information, as can be seen in the second panel of Figure 8, showing AMFs of the two algorithms synchronized with the OCRA-ROCINN cloud information. The use of the same cloud parameters reduces the mean difference from 0.146± 0.2 to 0.001± 0.1. For cloud fractions less than 40%, the AMFs calculated using FRESCO cloud parameters are about 5% higher than the AMFs calculated using OCRA/ROCINN cloud parameters.

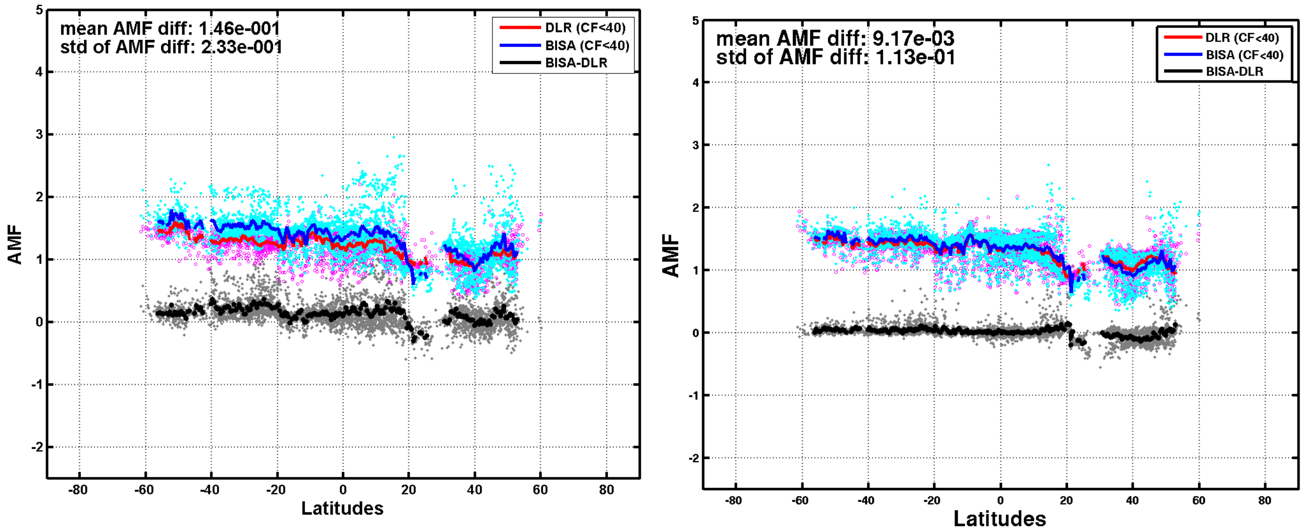

Figure 8. Comparison of total AMFs (for cloud fractions below 40%). In the first panel, AMFs are those calculated in GDP 4.4 and in the BIRA-IASB scientific algorithm. In the second panel, the BIRA-IASB AMFs are synchronized on the GDP using the same OCRA-ROCINN cloud information and the same albedo climatology.

Figure 9 shows the comparison between the H_2CO vertical columns for the April 4 orbit, calculated with the algorithms of BIRA-IASB and GDP 4.4. The first panel corresponds to the same ghost column correction for both algorithms, the second panel shows the modification of the GDP 4.4 to avoid negative vertical columns due to the ghost column correction. The differences between the vertical columns are shown in black. In both cases, there is a good agreement, with a mean difference below $4.5x10^{14}$ molec/cm² and a standard deviation under $2x10^{15}$ molec/cm², which is well under the mean uncertainty of one satellite observation of H_2CO. However, the modification of the ghost column correction in the GDP 4.4 could introduce a small positive bias between the scientific product and the GDP product for background conditions (this is part of ongoing research).

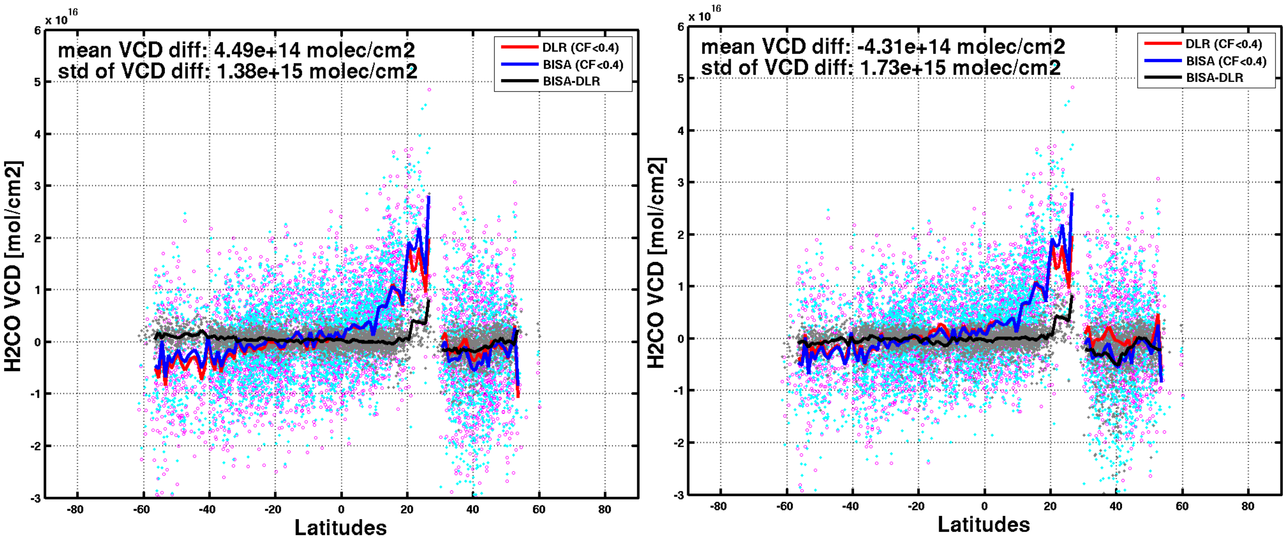

Figure 9. Comparison of H_2CO vertical columns retrieved from GDP 4.4 and from the adapted BIRA-IASB scientific algorithm, for one GOME-2 orbit of the 4th April 2007. In the first panel, the same ghost column correction has been applied in both algorithms. The second panel shows the modification of the GDP 4.4 algorithm (no ghost column correction for negative slant columns). The grey dots and black line correspond to the difference between GDP and BIRA-IASB H_2CO VCDs.

To go one step further in the verification, monthly averaged vertical columns need to be compared for selected emission regions, to exclude any geophysical discrepancy. The correlations of the GOME-2 H_2CO vertical column amounts retrieved from GDP 4.4 and from the BIRA-IASB scientific algorithm are shown in Figure 10. Note that both algorithms use identical DOAS settings (see Table 1). However in the calculation of the AMFs, different cloud products and albedo data bases are used, as explained in section D (see Table 2). Table 3 provides the coordinates of the regions selected for the comparison. The H_2CO VCD time series and the comparison with other satellite observations and ground-based measurements are shown in the next sections. The Figure 10 shows that the correlation between the GDP product and the scientific product is above 0.9 almost everywhere (with the exception of Europe and Indonesia, with respectively correlation coefficients of 0.6 and 0.7). In Europe, South China, India, South Asia, Guatemala, Indonesia and South Africa, the absolute H_2CO values agree within 15%, while in South-Eastern U.S., North Africa, Equatorial Africa, Amazonia and North Australia, the columns agree within 30%, which is good taking into account the error bars on the VCDs (De Smedt et al., 2008). The surface albedo and cloud products used, as well as the ghost column correction have important impacts on the resulting H_2CO data product. Preliminary tests have shown that in August 2007, in the Southeastern U.S. region, the OCRA/ROCINN cloud parameters results in formaldehyde columns 8% larger than those retrieved using FRESCO cloud parameters. In the same conditions, the modified ghost column correction results in 2% larger columns and the different surface albedo climatology results in a systematic difference of 12%. Future research work will focus on better assessing these effects, depending on the region and on the season.

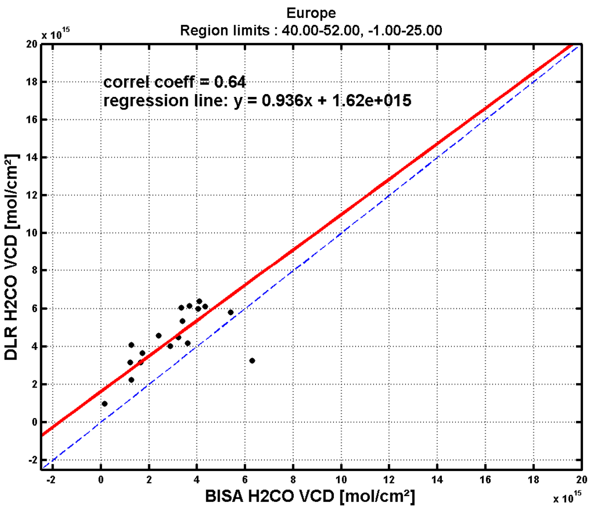
Europe
Region limits : 40.00-52.00, -1.00-25.00
correl coeff = 0.64
regression line: y = 0.936x + 1.62e+015
DLR H2CO VCD [mol/cm²]
BISA H2CO VCD [mol/cm²]

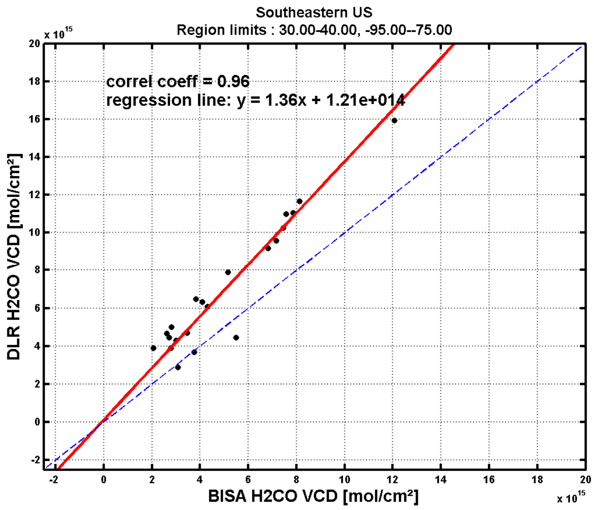
Southeastern US
Region limits : 30.00-40.00, -95.00--75.00
correl coeff = 0.96
regression line: y = 1.36x + 1.21e+014
DLR H2CO VCD [mol/cm²]
BISA H2CO VCD [mol/cm²]

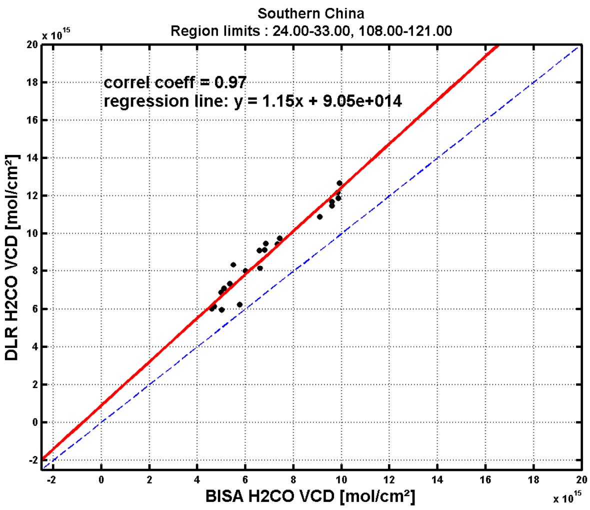
Southern China
Region limits : 24.00-33.00, 108.00-121.00
correl coeff = 0.97
regression line: y = 1.15x + 9.05e+014
DLR H2CO VCD [mol/cm²]
BISA H2CO VCD [mol/cm²]

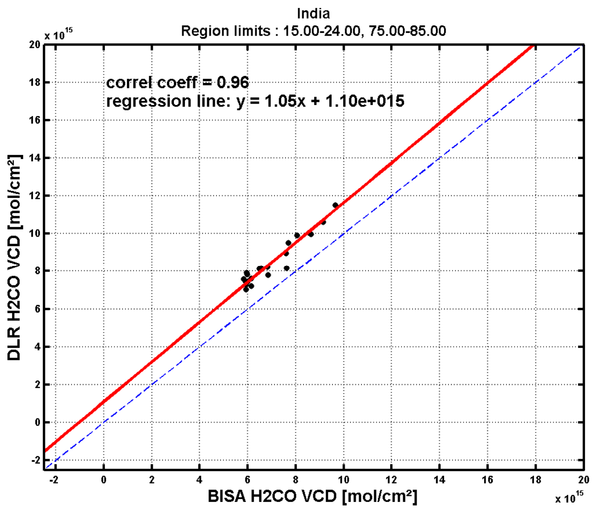
India
Region limits : 15.00-24.00, 75.00-85.00
correl coeff = 0.96
regression line: y = 1.05x + 1.10e+015
DLR H2CO VCD [mol/cm²]
BISA H2CO VCD [mol/cm²]

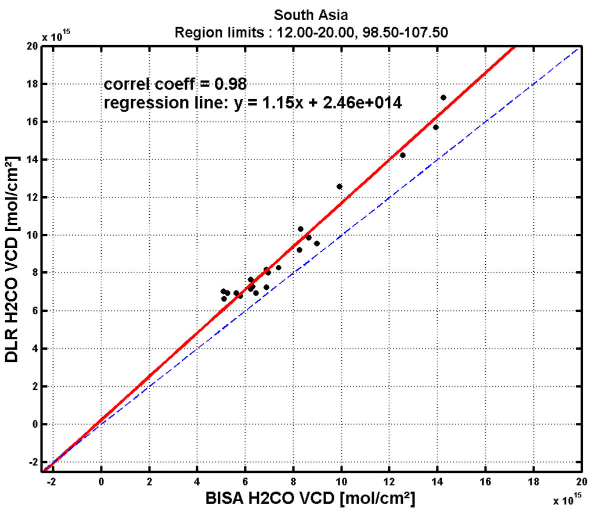
South Asia
Region limits : 12.00-20.00, 98.50-107.50
correl coeff = 0.98
regression line: y = 1.15x + 2.46e+014
DLR H2CO VCD [mol/cm²]
BISA H2CO VCD [mol/cm²]

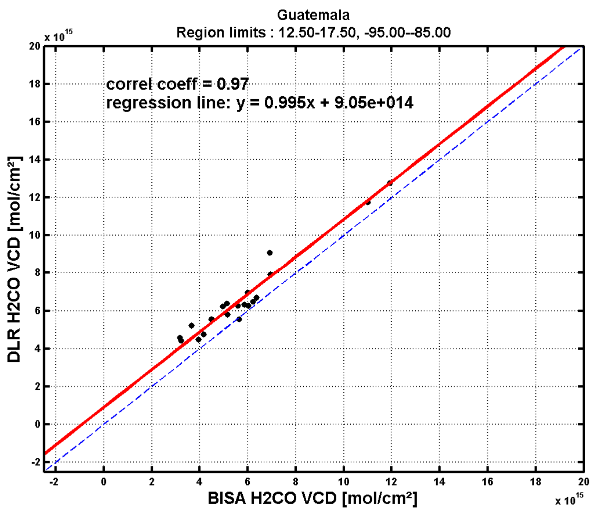
Guatemala
Region limits : 12.50-17.50, -95.00--85.00
correl coeff = 0.97
regression line: y = 0.995x + 9.05e+014
DLR H2CO VCD [mol/cm²]
BISA H2CO VCD [mol/cm²]

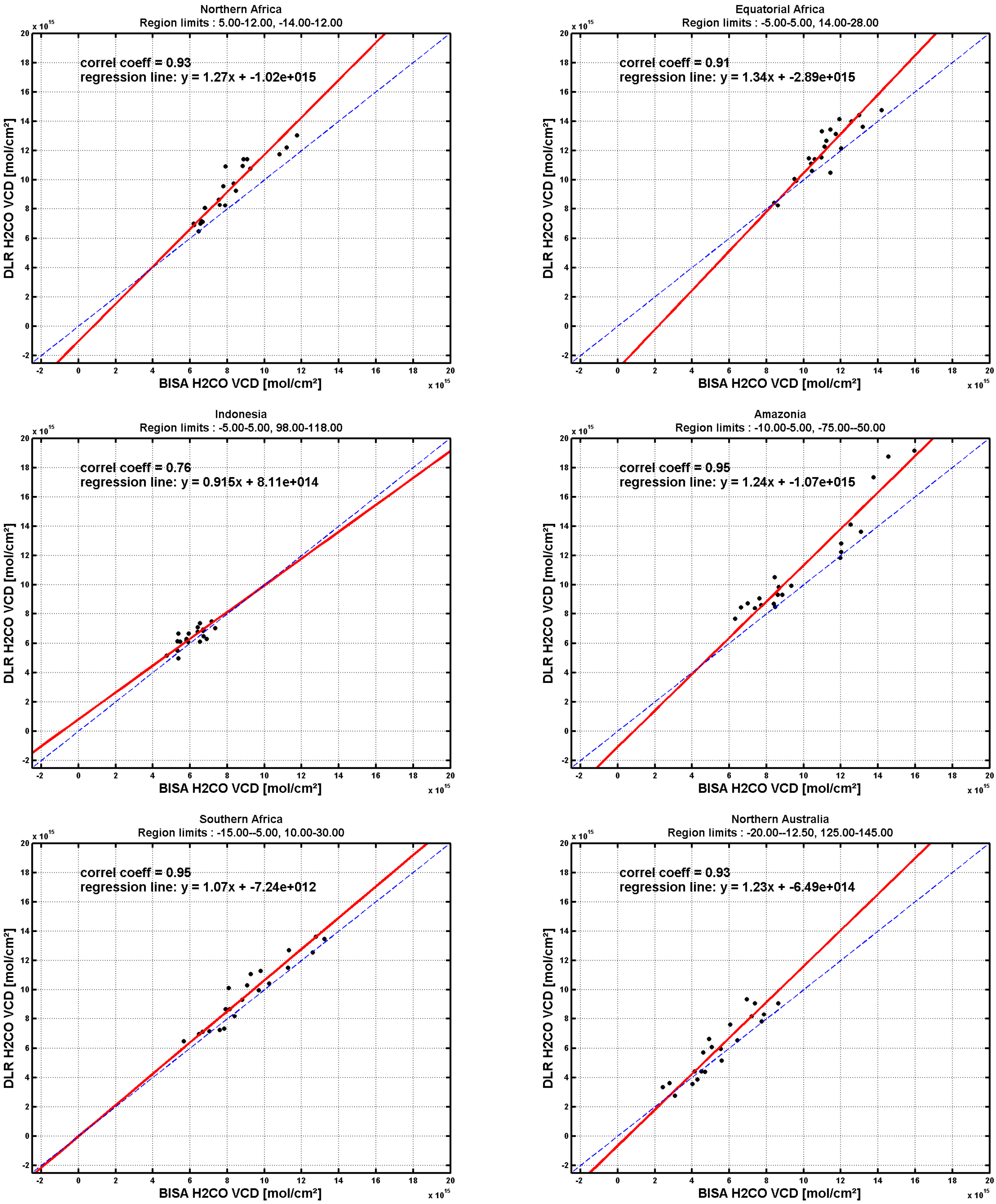

Figure 10. Correlations between the GDP product (DLR H_2CO VCD) and the scientific product (BIRA H_2CO VCD) of the monthly averaged H_2CO vertical columns in the regions of Table 2. Only pixels with cloud fraction below 40% and with solar zenith angles under 70° have been selected.

Table 3. List of regions used for the comparison with GOME and SCIAMACHY

Europe,	Lat: 40N - 52N	Lon: 1W - 25E
Southeastern_US,	Lat: 30N - 40 N	Lon: 75W - 95W
Southern_China,	Lat: 24N - 33 N	Lon: 108E - 121E
India,	Lat: 15N - 24N	Lon: 75E - 85E
South_Asia,	Lat: 12N - 20N	Lon: 98.5E - 107.5E
Guatemala,	Lat: 12.5N - 17.5N	Lon: 85W - 95W
Northern_Africa,	Lat: 12N - 20N	Lon: 98.5E - 107.5E
Equatorial_Africa,	Lat: 5S - 5N	Lon: 14E - 28E
Indonesia,	Lat: 5S - 5N	Lon: 98E - 118E
Amazonia,	Lat: 10S - 5N	Lon: 75W - 50W
Southern_Africa,	Lat: 15S - 5S	Lon: 10E - 30 E
Northern_Australia,	Lat: 20S - 12.5S	Lon: 125E - 145E

E. COMPARISON AGAINST SATELLITE DATA

H_2CO vertical column amounts derived from GOME and SCIAMACHY instruments have been produced at BIRA-IASB as part of the DUP/DUE TEMIS service (www.temis.nl). This 13-years data set has been used here for comparison with GOME-2 retrievals from the GDP 4.4 data set. Table 3 provides the coordinates of the regions selected for comparison.

GOME, SCIAMACHY and GOME-2 H_2CO vertical columns have been extracted above each site according to measurement periods available from the different data sets. Monthly averaged of pixels with cloud coverage below 40% and solar zenith angle under 70° are presented in Figure 11. A thorough description of the error estimation for GOME and SCIAMACHY is provided in De Smedt et al. (2008). A random and a systematic error component of the slant columns are estimated. The random error on the slant columns reaches 10^{16} molec./cm^2, whereas the systematic error, accounting for different sources of uncertainties (e.g. absorption cross-sections, inaccurate calibration, etc.), ranges from 2.5×10^{15} in tropical regions to 8.0×10^{15} molec./cm^2 at high latitudes. The error on the air mass factor calculations is estimated at 18% under clear sky conditions, but increases in the presence of clouds. On average, the total uncertainty on the monthly H_2CO vertical column ranges between 20 and 40% for regions with high signal to noise ratio. In the scientific GOME-2 H_2CO product, errors have been calculated following the same method. These values have been used in Figure 11 as an estimation of the errors on the GDP 4.4 columns. The geophysical consistency of the different satellite observations is highly satisfactory, taking into account the uncertainties on the vertical columns. These uncertainties increase with latitude and solar zenith angles (for example in Europe) and decrease when the emission levels increase, mainly in tropical regions. The seasonal variations, different for each region and emission source, are well reproduced with the 3 satellite instruments. In mid-latitude regions (Europe and South-Eastern U.S.), GOME-2 observations present a degradation in time due to the signal to noise ratio (S/N) loss of the instrument, which is mainly visible during the winter period when the H_2CO amount in the atmosphere is small and close to the detection limit of GOME-2.

The correlation between the H_2CO values as seen by SCIAMACHY and GOME-2 during the overlapping period is shown in Figure 12. As for the comparison with the scientific product, the correlation coefficient is above 0.9 almost everywhere. Europe, India and Indonesia present correlation coefficients of respectively 0.7, 0.8 and 0.2. The very poor coefficient in Indonesia could be explained by the quasi non-emission period between 2007 and 2009, making difficult the estimation of a correlation (see Figure 11). In South-Eastern U.S., South China, India, Guatemala, Northern Africa, Equatorial Africa and South Africa the absolute H_2CO values agree within 15% between SCIAMACHY and GOME-2, which is highly satisfactory. In other regions (Europe, South Asia, Indonesia, Amazonia and Northern Australia), GOME-2 present higher values than SCIAMACHY, the GOME-2 values being up to 50% higher than the ones observed by SCIAMACHY. An overestimation of the formaldehyde columns by GOME-2 is possible but it should not be forgotten that SCIAMACHY observations have their own uncertainties. External independent validation data are needed to draw conclusions on the quality of the H_2CO satellite observations.

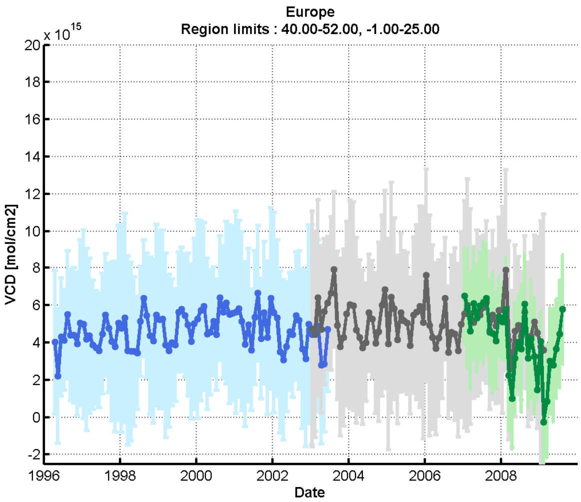
Europe
Region limits : 40.00-52.00, -1.00-25.00
x 10^15
VCD [mol/cm2]
Date

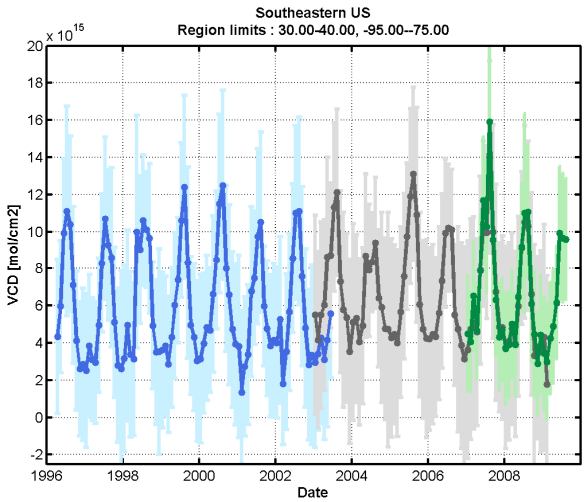
Southeastern US
Region limits : 30.00-40.00, -95.00--75.00
x 10^15
VCD [mol/cm2]
Date

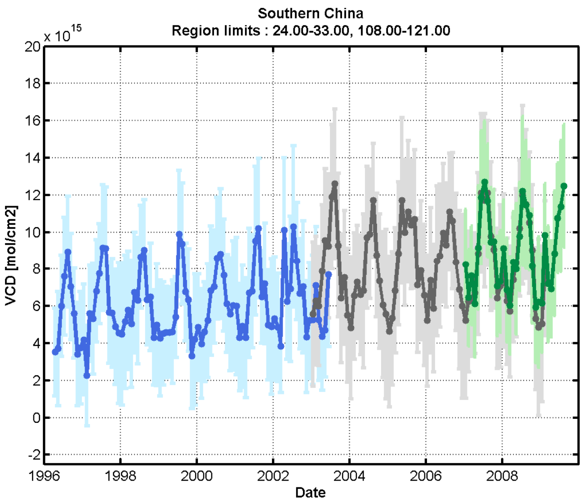
Southern China
Region limits : 24.00-33.00, 108.00-121.00
x 10^15
VCD [mol/cm2]
Date

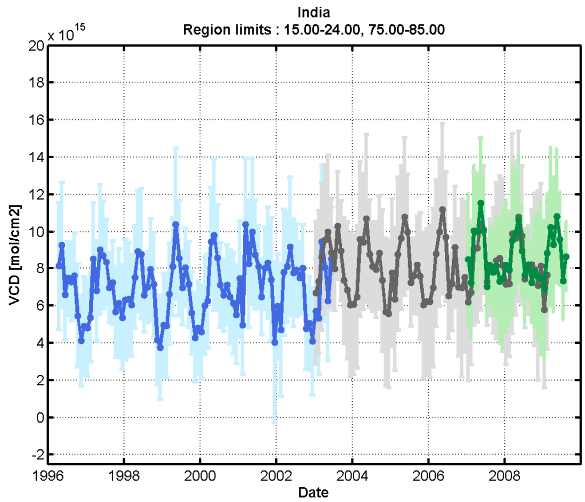
India
Region limits : 15.00-24.00, 75.00-85.00
x 10^15
VCD [mol/cm2]
Date

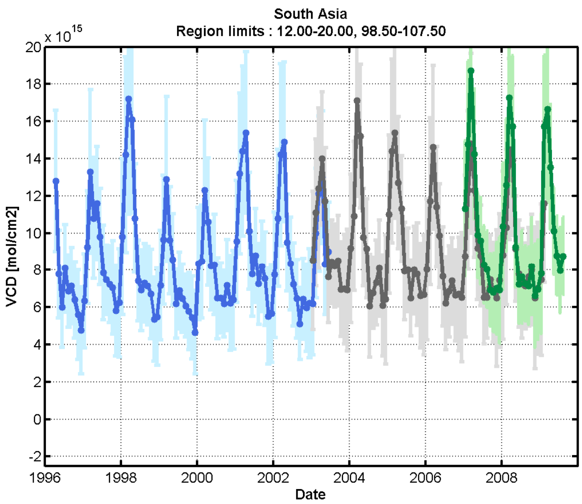
South Asia
Region limits : 12.00-20.00, 98.50-107.50
x 10^15
VCD [mol/cm2]
Date

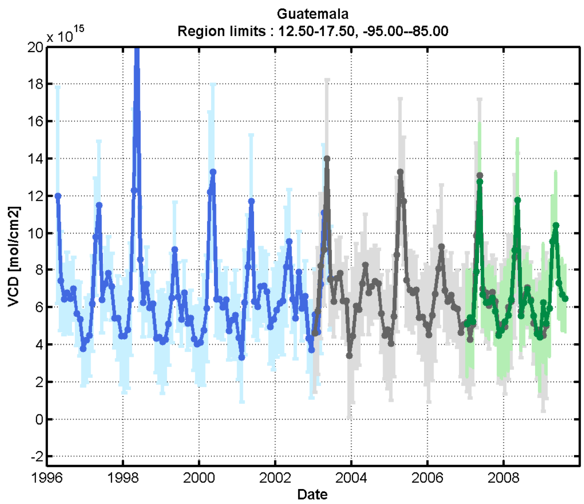
Guatemala
Region limits : 12.50-17.50, -95.00--85.00
x 10^15
VCD [mol/cm2]
Date

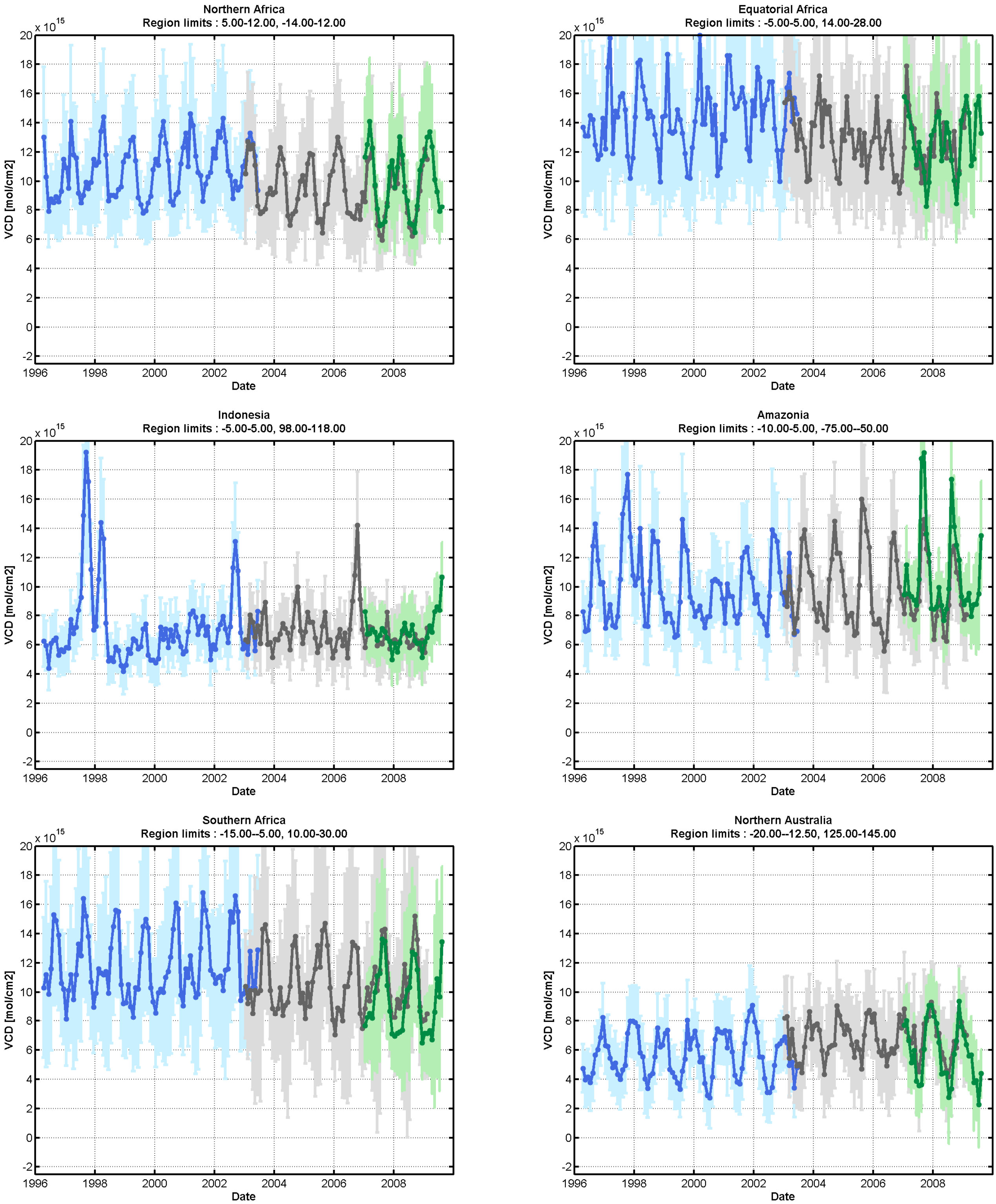

Figure 11. Comparison of time-series of monthly averaged H_2CO vertical columns retrieved from GOME (in blue), SCIAMACHY (in grey) and the GDP GOME-2 product (in green) over the 2007-2009 period, in the same regions as in Fig. 8. Only pixels with cloud fraction below 40% and solar zenith angles below 70° have been selected.

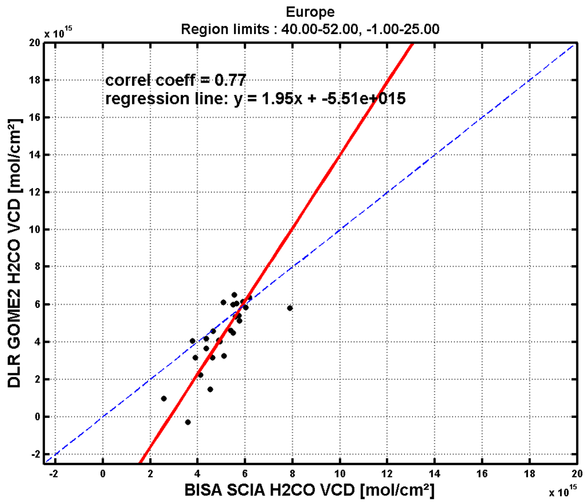
Europe
Region limits : 40.00-52.00, -1.00-25.00
correl coeff = 0.77
regression line: y = 1.95x + -5.51e+015
DLR GOME2 H2CO VCD [mol/cm²]
BISA SCIA H2CO VCD [mol/cm²]

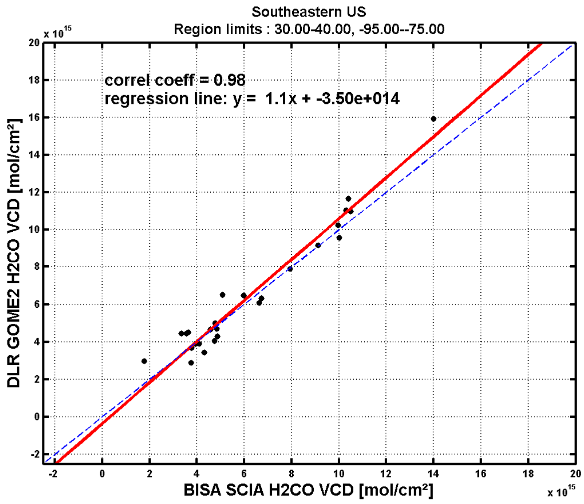
Southeastern US
Region limits : 30.00-40.00, -95.00--75.00
correl coeff = 0.98
regression line: y = 1.1x + -3.50e+014
DLR GOME2 H2CO VCD [mol/cm²]
BISA SCIA H2CO VCD [mol/cm²]

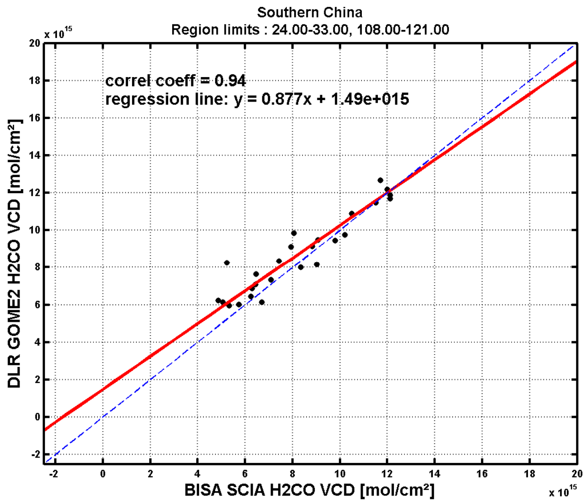
Southern China
Region limits : 24.00-33.00, 108.00-121.00
correl coeff = 0.94
regression line: y = 0.877x + 1.49e+015
DLR GOME2 H2CO VCD [mol/cm²]
BISA SCIA H2CO VCD [mol/cm²]

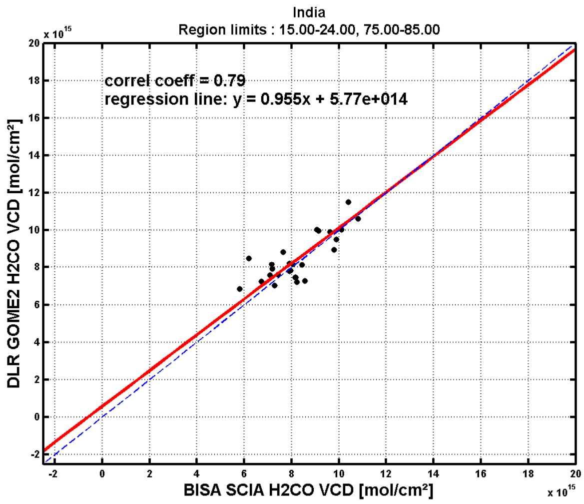
India
Region limits : 15.00-24.00, 75.00-85.00
correl coeff = 0.79
regression line: y = 0.955x + 5.77e+014
DLR GOME2 H2CO VCD [mol/cm²]
BISA SCIA H2CO VCD [mol/cm²]

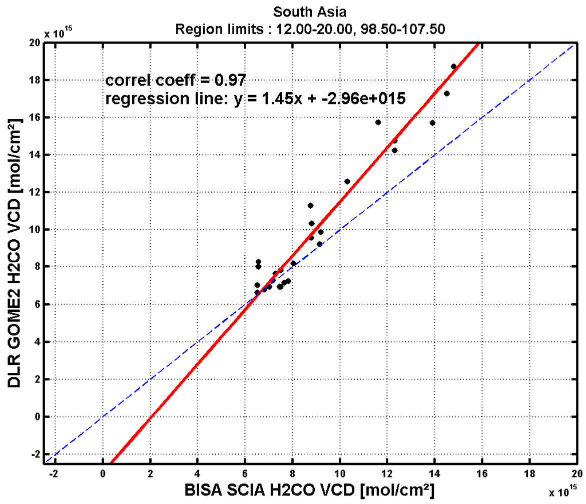
South Asia
Region limits : 12.00-20.00, 98.50-107.50
correl coeff = 0.97
regression line: y = 1.45x + -2.96e+015
DLR GOME2 H2CO VCD [mol/cm²]
BISA SCIA H2CO VCD [mol/cm²]

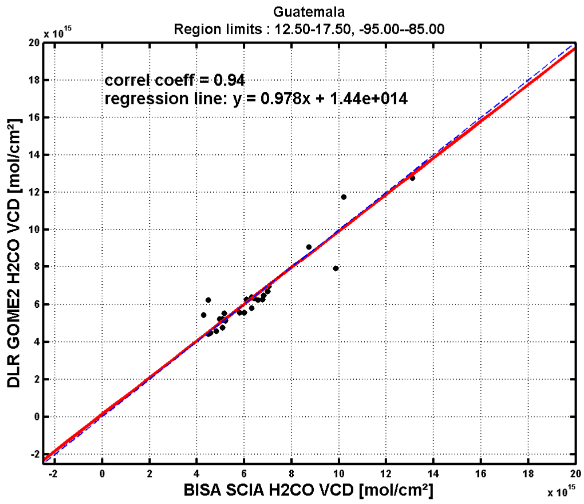
Guatemala
Region limits : 12.50-17.50, -95.00--85.00
correl coeff = 0.94
regression line: y = 0.978x + 1.44e+014
DLR GOME2 H2CO VCD [mol/cm²]
BISA SCIA H2CO VCD [mol/cm²]

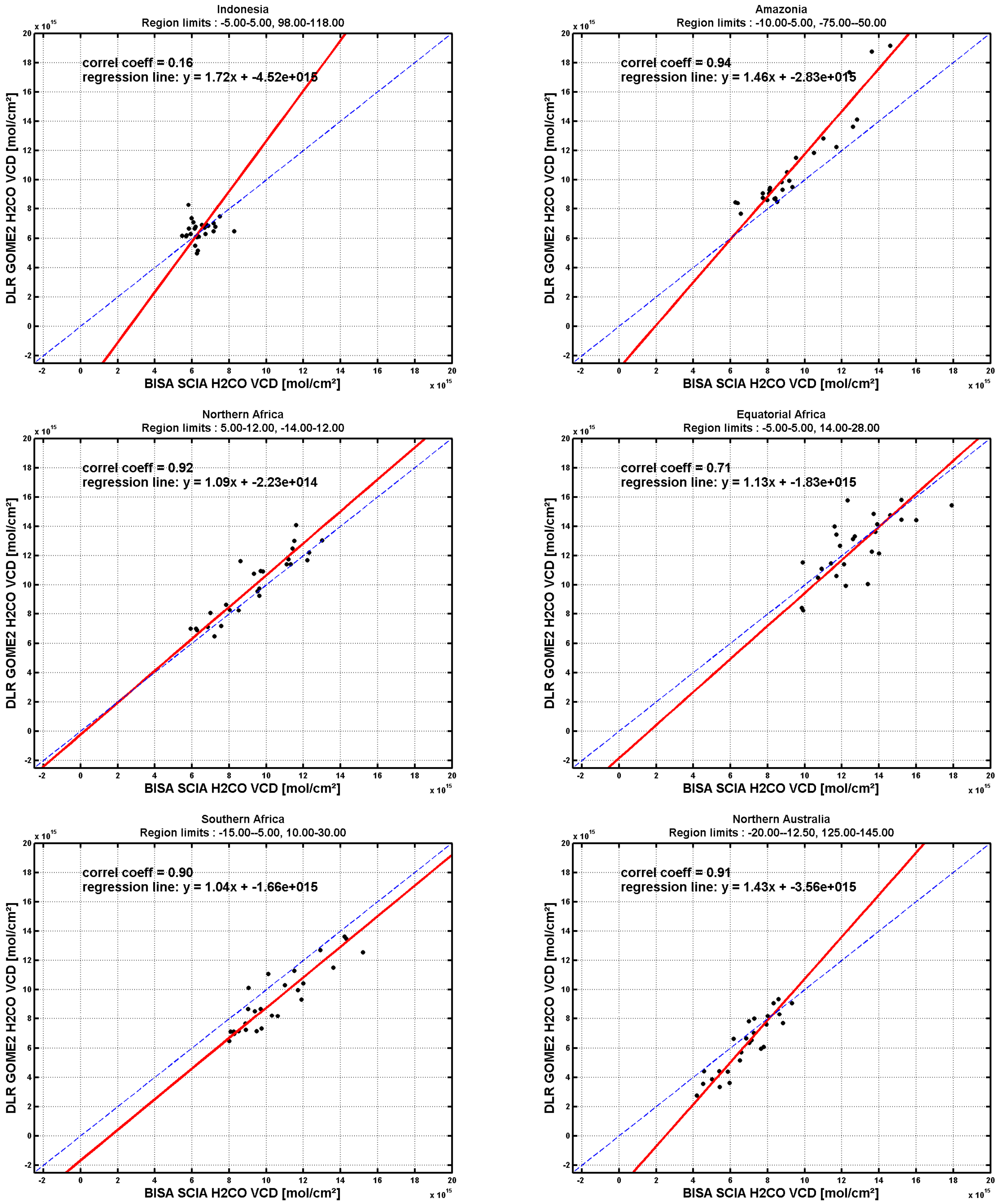

Figure 12. Correlations between the GOME-2 GDP product (DLR H_2CO VCD) and the SCIAMACHY product (BIRA SCIA H_2CO VCD) of the monthly averaged H_2CO vertical columns in the same regions as in Fig. 9, for overlapping periods.

F. COMPARISON AGAINST GROUND-BASED MEASUREMENTS

The first available time series of ground-based FTIR formaldehyde observations in the tropics can be used for the validation of the satellite H_2CO columns (Vigouroux et al., 2009). The observation site was Reunion Island in the Indian Ocean. This station is part of the Network for the Detection of Atmospheric Composition Change (NDACC). The Reunion station is one of the very few NDACC stations located at southern tropical or subtropical latitudes. In preparation to a permanent installation planned for 2011, three campaigns of FTIR measurements have been performed by BIRA-IASB, in October 2002, from August to October 2004, and from May to November 2007. The FTIR inversion algorithm is based on the Optimal Estimation Method (Rodgers, 2000) by which information about the vertical distribution of the target gases can be derived. The error on the FTIR columns is 20% (Vigouroux et al., 2009). Reunion Island, being a small island located in the Indian Ocean, can be seen as a remote marine site where the methane oxidation is the dominant formaldehyde source. Figure 13 presents the comparison of the monthly averaged SCIAMACHY and GOME-2 columns, within a radius of 500 km around the island, with the monthly averaged FTIR columns during the last two campaigns. The seasonal variation of formaldehyde is well reproduced and we find no bias between the satellite and the FTIR, which validates our reference sector correction.

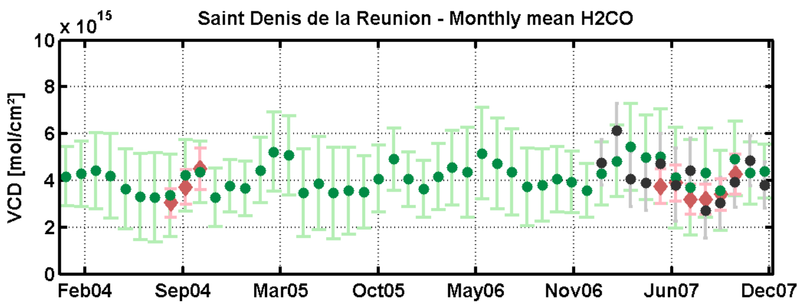

Figure 13. Comparison between monthly averaged SCIAMACHY (green dots) and GDP 4.4 GOME-2 (black dots) formaldehyde monthly means, with results from 2 FTIR campaigns at Reunion Island (pink diamonds).

In mid-latitude regions, the new MAX-DOAS instrument developed at BIRA-IASB can be used for the validation of formaldehyde tropospheric columns. First, the instrument was installed in Beijing (China) at IAP/CAS from June 2008 until April 2009. Just after, the instrument was moved to Cabauw (The Netherlands) for the CINDI campaign during the months of June and July 2009. The instrument has been designed using a multi-axis geometry. The light is collected at different elevation angles, from the horizon to the zenith. This allows separating the stratospheric and tropospheric contributions. Assuming that the H_2CO layer is below the scattering altitude, a geometrical approximation can be used to obtain tropospheric vertical columns. We estimate that the error on the columns can reach up to 50%. A more sophisticated and accurate retrieval algorithm is currently under development at BIRA-IASB.

Figure 14 presents GDP 4.4 GOME-2 monthly mean vertical columns extracted in a radius of 200 km around Beijing. These are compared to SCIAMACHY H_2CO columns and to monthly averaged MAX-DOAS tropospheric columns measured at the satellite overpass time. The GOME-2 columns show a good agreement with ground-based results in Beijing although they tend to be over-estimated in summer 2008, while they are generally underestimated during the winter. The correlation between the GDP 4.4 GOME-2 columns and the observations of the MAX-DOAS is presented in Figure 15. The regression line shows that the GDP 4.4 GOME-2 columns are 26% higher than the MAX-DOAS observations, which is within the uncertainties of the measurements.

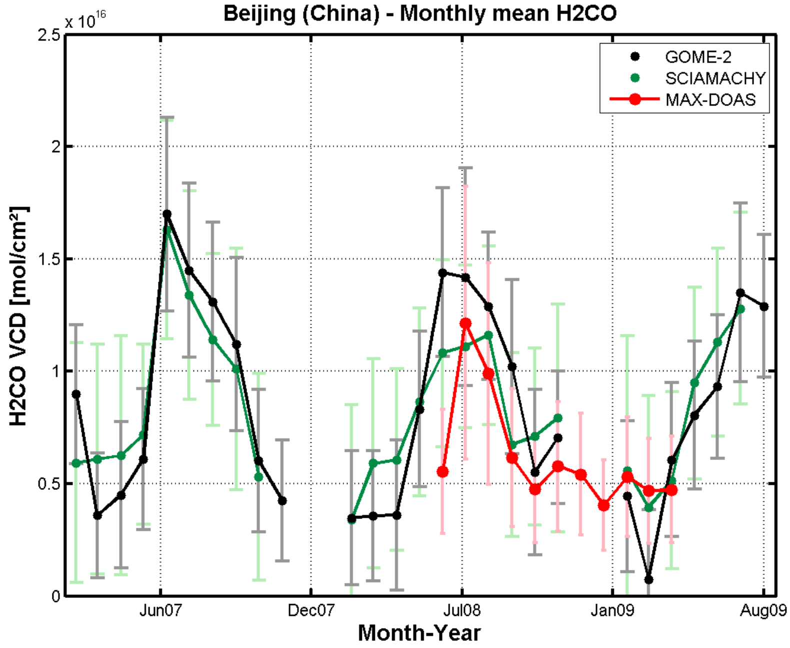

Figure 14. Monthly averaged SCIAMACHY (in green) and GOME-2 (in black) formaldehyde columns compared with MAX-DOAS measurements in Beijing. MAXDOAS data are extracted at the satellite overpass time (in red).

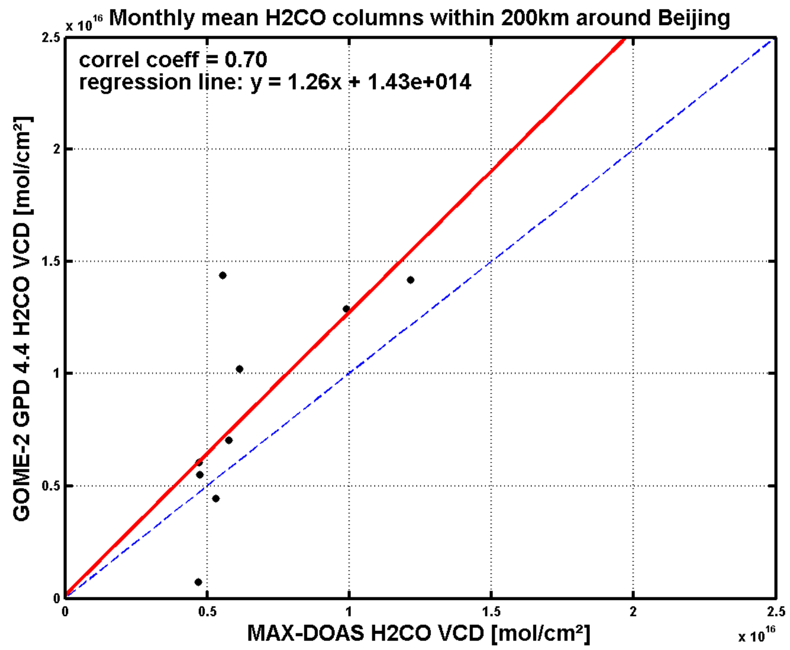

Figure 15. Correlation between the GOME-2 GDP 4.4 formaldehyde columns and the MAX-DOAS measurements in Beijing.

Figure 16 presents the GDP 4.4 GOME-2 monthly H_2CO, in a radius of 100 km around Cabauw, compared with the monthly averaged MAX-DOAS tropospheric column at the satellite overpass time. In Cabauw, GOME-2 H_2CO columns are 45% lower than the to the MAX-DOAS columns. In Europe, the emission levels of formaldehyde are relatively low, and the H_2CO signal is close to the detection limit of the satellite.

However, the improved coverage of GOME-2 compared to SCIAMACHY improves the signal to noise ratio of the monthly averaged H_2CO columns. This allows detecting the seasonal variation of the formaldehyde columns over Europe. Again, the agreement between the GOME-2 observations and the MAX-DOAS columns is within the error bars of the measurements.

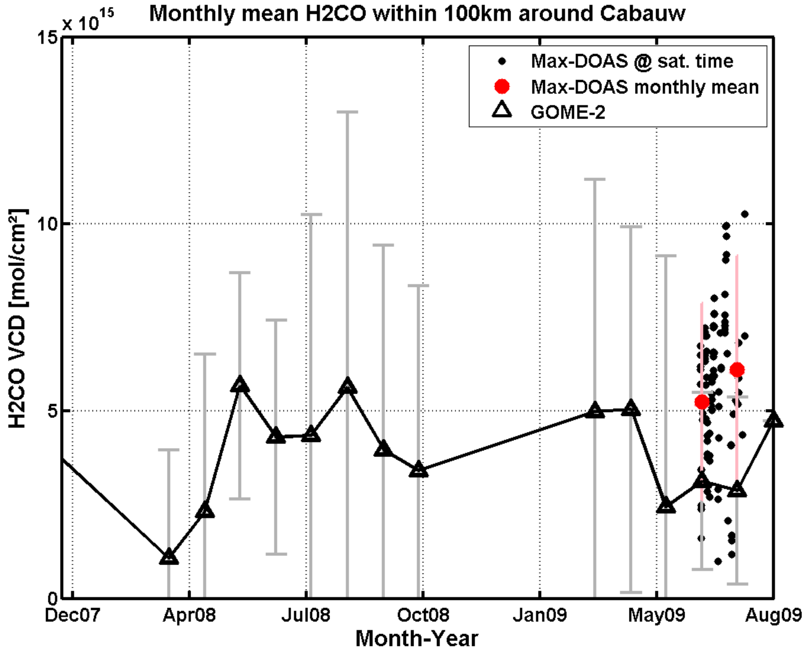

Figure 16. Monthly averaged GDP 4.4 GOME-2 (black triangles) formaldehyde columns compared with the MAX-DOAS measurements in Cabauw. Black dots are the ground-based observations at satellite overpass time and red dots are their monthly average.

G. CONCLUSIONS

GOME-2 H_2CO retrieval settings derived from scientific developments at BIRA-IASB have been adapted for integration in the UPAS operational environment system at DLR.

Verifications of the slant columns, of the reference sector correction, the air mass factors and vertical columns have been conducted on a selection of GOME-2 orbits. Monthly averaged columns retrieved with GDP 4.4 have been calculated for a selection of emission regions between 2007 and August 2009 and compared with results from an adapted version of the scientific product that matches the settings adopted for the operational UPAS processor. Although the GDP 4.4 H_2CO columns generally tend to be slightly higher than those of the adapted scientific product, both data products show a very good level of consistency when considering the typical uncertainties on H_2CO retrieval. Vertical columns are in agreement to better than 30% in average. Our study indicates that cloud effects have an important impact of the resulting H_2CO data product. Future research work will focus on better assessing these effects in relation to the cloud parameters used as an input for the trace gas retrieval.

In order to validate the GOME-2 OTO/HCHO product, comparisons have been performed with correlative data sets from previous satellite instruments (GOME and SCIAMACHY) as well as with ground-based measurements available at Reunion Island (Southern tropics), Beijing (Eastern China) and Cabauw (The Netherlands). The comparison with GOME and SCIAMACHY observations is good overall although GOME-2 presents higher values in some regions. In average, the GOME-2 values are 25% higher than the concordant SCIAMACHY observations. This level of agreement is better than the error bars provided for the different satellite observations. In comparison to GOME and SCIAMACHY, the GOME-2 results from both GDP 4.4 and the scientific algorithm generally tend to be of reduced quality in winter at mid-latitudes, due to the high solar zenith angle conditions encountered at the local time of the METOP orbit (approximately 9:30). Concerning comparisons with ground-based measurements, we find that the GDP 4.4 GOME-2 H_2CO columns are overestimated over Beijing in summer 2008, and underestimated in winter. The correlation between the GDP 4.4 GOME-2 columns and the MAX-DOAS observations is 0.7, and the regression line presents a slope of 26%. Comparisons with Cabauw measurements in spring 2009 indicate that satellite retrievals might be underestimated by about 45% in these conditions. Note however that such validation results are still compliant with the target accuracy (50%). Nevertheless investigations are currently performed at BIRA-IASB to improve both the current scientific data product and the accuracy and representativity of ground-based validation data sets.

Based on the validation with ground-based measurements and the comparisons with correlative GOME and SCIAMACHY data, we concluded that the current GOME-2 OTO/HCHO column product already fulfill the user requirements in terms of accuracy, as stated in the Product Requirements Document (Target accuracy: 50%; Optimal: 30%) and can be declared as fully operational.

For further validation of the H_2CO satellite observations, more validation sites are needed, as well as longer observation campaigns.

H. REFERENCES

Bogumil, K., J. Orphal, T. Homann, S. Voigt, P. Spietz, O.C. Fleischmann, A. Vogel, M. Hartmann, H., Bovensmann, J. Frerick, and J.P. Burrows, Measurements of molecular absorption spectra with the SCIAMACHY pre-flight model: Instrument characterization and reference data for atmospheric remote sensing in the 230-2380 nm region, J. Photochem. Photobiol. A.: Photochem., 157, 167-184, 2003.

Brion, J., Chakir, A., Charbonnier, J., Daumont, D., Parisse, C. and Malicet, J., Absorption spectra measurements for the ozone molecule in the 350-830 nm region, J. Atmos. Chem., 30, 291-299, 1998.

Brion, J., Chakir, A., Daumont, D. and Malicet, J., High-resolution laboratory absorption cross section of O3. Temperature effect, Chem. Phys. Lett., 213 (5-6), 610-512, 1993.

Chance, K., P.I. Palmer, R.J.D. Spurr, R.V. Martin, T.P. Kurosu, and D.J. Jacob, Satellite observations of formaldehyde over North America from GOME, Geophys. Res. Lett., 27, 21, 3461-3464, 2000.

De Smedt I, Müller J.-F., Stavrakou T, van der A, R., Eskes, H. and Van Roozendael, M., Twelve years of global observation of formaldehyde in the troposphere using GOME and SCIAMACHY sensors. Atmos. Chem. Phys., 8 (16), 4947-4963, 2008.

Fleischmann, O. C., Hartmann, M., Burrows J. P., and Orphal, J.: New ultraviolet absorption cross-sections of BrO at atmospheric temperatures measured by time-windowing Fourier transform spectroscopy, J. Photochem. Photobiol. A, 168, 117–132 , 2004.

Koelemeijer, R. B. A., P. Stammes, J. W. Hovenier, and J. F. de Haan, Global distributions of effective cloud fraction and cloud top pressure derived from oxygen A band spectra measured by the Global Ozone Monitoring Experiment: comparison to ISCCP data, J. Geophys. Res., 107(D12), 4151, doi:10.1029/2001JD000840, 2002.

Koelemeijer, R. B. A., J. F. de Haan, and P. Stammes, A database of spectral surface reflectivity in the range 335-772nm derived from 5.5 years of GOME observations, J. Geophys. Res., 108(D2), 4070, doi:10.1029/2002JD002429, 2003.

Martin, R.V., K. Chance, D. J. Jacob, T. P. Kurosu, R. J. D. Spurr, E.Bucsela, J. F. Gleason, P. I. Palmer, I. Bey, A. M. Fiore, Q. Li, R. M. Yantosca, and R. B. A. Koelemeijer, An improved retrieval of tropospheric nitrogen dioxide from GOME, J. Geophys. Res., 107(D20), 4437, doi:10.1029/2001JD001027, 2002.

Mayer, B. and Kylling, A., Technical note: The libRadtran software package for radiative transfer calculations – description and examples of use, Atmos. Chem. Phys., 5, 1855-1877, 2005.

Meller, R. and Moortgat, G. K., Temperature dependence of the absorption cross sections of formaldehyde between 223 and 323K in the wavelength range 225–375 nm, J. Geophys. Res., 105(D6), 7089–7101, 2000.

Palmer, P. I., D. J. Jacob, K. Chance, R. V. Martin, R. J. D. Spurr, T. P. Kurosu, I. Bey, R. Yantosca, A. Fiore, and Q. Li, Air-mass factor formulation for spectroscopic measurements from satellites: application to formaldehyde retrievals from GOME, J. Geophys. Res., 106(D13), 14539-14550, 10.1029/2000JD900772, 2001.

Richter, A. and T. Wagner, Diffuser plate spectral structures and their influence on GOME slant columns, Tech. rep., Inst. Env. Phys., Univ. Bremen and Inst. Env. Phys., Univ. Heidelberg, 2001.

Rodgers, C. D., Inverse methods for atmospheric sounding, Theory and Practice, Series on Atmospheric, Oceanic and Planetary Physics-Vol. 2, World Scientific, 2000.

Stavrakou, T., Müller, J.-F., De Smedt, I., Van Roozendael, M., van der Werf, G. R., Giglio, L., and Guenther, A.: Evaluating the performance of pyrogenic and biogenic emission inventories against one decade of space-based formaldehyde columns, Atmos. Chem. Phys., 9, 20 1037–1060, 2009a.

Stavrakou, T., Müller, J.-F., De Smedt, I., Van Roozendael, M., van der Werf, G. R., Giglio, L., and Guenther, A.: Global emissions of non-methane hydrocarbons deduced from SCIAMACHY formaldehyde columns through 2003–2006, Atmos. Chem. Phys., 9, 3663–3679, 25 2009b.

Vandaele, A.C., Hermans, C., Fally, S., Carleer, M., Colin, R., Mérienne, M.-F. and Jenouvrier, A., High-resolution Fourier transform measurement of the NO2 visible and near-infrared absorption cross-section: Temperature and pressure effects, J. Geophys. Res. 107, D18, 4348, doi:10.1029/2001JD000971, 2002.

Vigouroux.C, F. Hendrick, T. Stavrakou, B. Dils, I. De Smedt, C. Hermans, A. Merlaud, F. Scolas, C. Senten, G. Vanhaelewyn, S. Fally, M. Carleer, J.-M. Metzger, J.-F. Mueller, M. Van Roozendael1, and M. De Maziere: Ground-based FTIR and MAX-DOAS observations of formaldehyde at Reunion Island and comparisons with satellite and model data, Atmos. Chem. Phys., 9, 9523–9544, 2009.

Wang, P., Stammes, P., van der A, R., Pinardi, G., and van Roozendael, M., FRESCO+: an improved O2 A-band cloud retrieval algorithm for tropospheric trace gas retrievals, Atmos. Chem. Phys., 8, 6565-6576, 2008.